Coupling of apical-basal polarity and PCP to interpret the Wnt signaling gradient and orient feather branch

Jianqiong Lin and Zhicao Yue*

Institute of Life Sciences, Fuzhou University, Fuzhou, Fujian, China

*Author for correspondence (zyue@fzu.edu.cn)

Zhicao Yue, PhD

Professor & Director
Institute of Life Sciences
Fuzhou University
2 Xue Yuan Road, University Campus
Fuzhou, Fujian, China 350116
Email: zyue@fzu.edu.cn
Tel: 86-591-22865094

ABSTRACT

To sense a global directional cue and orient cell growth is crucial in tissue morphogenesis. An anterior-posterior gradient of Wnt signaling controls the helical growth of feather branches (barbs), thus the formation of bilateral feathers. However, it remains unclear how the keratinocytes sense this gradient and orient barb growth. Here we show that due to feather branching, the global Wnt gradient is subdivided into periodic barbs. Within each barb, the anterior barbule plate cells tilt before the posterior cells. The core PCP gene *Prickle1* is involved, as knockdown of its expression resulted in no cell shape change and no barb tilting. Furthermore, perturbation of the Wnt gradient leads to diffusive Prickle1 expression, and loss of barb orientation. Finally, the asymmetric distribution of Wnt6/Fzd10 is coordinated by the apical-basal polarity of the barbule plate keratinocytes, which is in turn regulated by the Par3/aPKC machinery. Our data elucidate a new mechanism through which the global Wnt signaling gradient is interpreted locally to construct complex spatial forms.

KEY WORDS: Wnt signaling, Morphogen gradient, Planar cell polarity, Apical-basal polarity, Prickle1, Feather

Summary: The feather keratinocytes interpret the global Wnt signaling gradient through coupling with the local apical-basal polarity cue and change their shape accordingly.

INTRODUCTION

Directional sensing is essential for the construction of appropriate spatial forms. This is often achieved through the formation and interpretation of a signaling gradient in the morphogenetic field (Yang and Mlodzik, 2015; Aw and Devenport, 2017; Sagner and Briscoe, 2017; Lander, 2007). A classical example is the Drosophila wing, where the directions of epithelial hairs and bristles are coordinated globally via a core mechanism termed planar cell polarity (PCP), in response to a supposed global signaling gradient cue (Yang and Mlodzik, 2015; Bayly and Axelrod, 2011; Zallen, 2007). Similar mechanism has been shown to control limb bud elongation in higher vertebrates (Gao et al., 2011; Gao and Yang, 2013).

It remains highly controversial as to how the morphogen gradient is established and interpreted (Akiyama and Gibson, 2015; Nahmad and Lander, 2011). Although passive diffusion could be a driving force, recent work suggested that the Wnt ligands do not diffuse; rather they remain cell bound and distribute only with cell division (Farin et al., 2016; Boutros and Niehrs, 2016). Alternatively, the signaling molecules can be transported via long cyto-projections, the so-called cytoneme structure (Kornberg and Roy, 2014; Hamada et al., 2014; Sanders et al., 2013). Therefore, it is of fundamental importance to clarify how cells sense and interpret the signaling gradient to coordinate cell shape change and pattern formation.

Avian feathers are composed of terminally differentiated keratinocytes with complex structures (Lucas and Stettenheim, 1972; Chen et al., 2015; Lin et al., 2013; Yu et al., 2004; Feo et al., 2016; Prum, 2005; Prum and Williamson, 2001). A feather can be either bilaterally symmetric, which has a central axis (rachis) where branches (barbs) insert, or radially symmetric, which has only a short calamus where barbs attach (Chen et al., 2015; Yu et al., 2004; Prum, 2005; Yue et al., 2006). Our previous work has demonstrated that the emergency of an anterior-posterior Wnt signaling gradient in the developing feather follicle breaks the symmetry and induces tilting of barbs, thus the formation of bilaterally symmetric feather (Yue et al., 2006). It remains unclear how this gradient is interpreted by feather keratinocytes, and whether the PCP pathway is involved.

In recent years, we have developed methods to overexpress or knockdown gene expression in the feather follicle through lentiviral-mediated gene transfer *in vivo* with high efficiency (Chu et al., 2014; Chen et al., 2014; Xie et al., 2015; Cheng et al., 2018). In our effort to screen gene functions in the feather follicle, we found that the core PCP gene *Prickle1 (Pk1)* controls directional sensing in feather development. Further work revealed that the Wnt/Fzd signaling is involved, which in turn is controlled by the apical-basal polarity of feather keratinocytes, namely Par3/aPKC. This work sheds new light on how the global signaling gradient is interpreted locally to build complex 3D structures.

RESULTS

Coordinated cell shape change tilts feather branch

The two basic feather forms differ in their symmetric levels (Fig. 1A and 1B). The radially symmetric feathers have no central rachis, and the branches (barbs) are perpendicularly attached to the calamus. In bilaterally symmetric feathers, there is a central rachis, and the barbs are helically tilted toward the rachis (Yue et al., 2006). Histologically, each barb is composed of two columns of marginal plate cells in the peripheral, two columns of barbule plate cells with distinct elongated shape, which are separated by axial plate cells. The anterior barbule plate cells are tilted before the posterior barbule plate cells, with no obvious tilting in radially symmetric feathers (Fig. 1C and 1D). This change of cell shape is a gradual process, with characteristic elongated barbule plate cells even in radial feathers (Fig. 1E and Fig. S1; see Fig. S2 for the quantification of barbule plate cell parameters).

We wonder how this change in cell shape is translated into tilting of the feather branches. The tilting of the anterior barbule plate cells leads to an anterior expansion of the barb, which creates a tangential disparity, d_A-d_P (Fig. 1D). The calculated tilting angle is $tg\sigma = (d_A-d_P)/h$, where h is the height of the barb. We then measured the actual tilting (helical) angle of barbs in feather development (Fig. 1F). It turns out that the calculated angle σ fits well with the helical angle θ (Fig. 1F). Alternatively, it is also possible that θ is achieved through the cumulative effect of barbule cell tilting. That is, σ does not necessarily always correspond to θ, but cumulatively contributes to θ. Nonetheless, the coordinated cell shape change underlies the tilting of feather branches.

The core PCP gene *Pk1* controls cell shape change and barb tilting in feather development

In an effort to systematically dissect gene functions in feather development, we performed a RNAi screening using our established method of lentiviral-mediated gene knockdown *in vivo* (Chu et al., 2014; Chen et al., 2014; Xie et al., 2015; Cheng et al., 2018). We found that the core PCP gene *Pk1* controls feather cell shape change and bilateral feather formation (Fig. 2). *Pk1* is expressed in a graded pattern, with higher expression in the anterior follicle, similar to the pattern of Wnts (Yue et al., 2006 and Fig. 3). In each barb ridge, *Pk1* mRNA does not show a clear enrichment pattern (Fig. 2A). However, when examined by a specific antibody (Fig. S3), Pk1 is initially homogenous which then enriched in the barbule plate cells facing the axial plate (Fig. 2B; quantified in Fig. 2D). This polarized distribution suggests that *Pk1* may regulate cell shape change in feather development.

We then examined the functional role of *Pk1* in feather development. The RNAi knockdown efficiency for *Pk1* is about 90% when examined in DF-1 chicken fibroblast cells and about 80% in vivo (Fig. S4). When the RNAi virus was locally injected into the developing feather follicle, the barbule plate cells were unable to undergo the programmed shape change (Fig. 2C; quantified in Fig. 2D). Knockdown of *Pk1* expression moderately reduced cell proliferation, as shown by PCNA staining (Fig. 2E). The impact of *Pk1* knockdown was documented at both the whole mount level and the final feather morphology level. Local injection of the RNAi virus led to perpendicular barbs which lose their coordinated tilting toward the rachis (Fig. 2F, 2G). At the final feather morphology level, the perturbed feathers show transition toward radial symmetry (Fig. 2H). Together, these data suggest that the core PCP gene *Pk1* regulates cell shape change and barb tilting in feather development.

The Wnt/Fzd signaling controls Pk1 asymmetric distribution and cell shape change

We wonder if the polarized distribution and function of Pk1 is down-stream and thus is regulated by the Wnt/Fzd signaling. In our previous effort to map gene expression in the feather follicle (Chu et al., 2014; Cheng et al., 2018; GSE42017 and GSE110591), we have found that the Wnt ligands expressed in the feather epithelium are mainly Wnt6 and Wnt5a. In situ hybridization revealed that both show an anterior-posterior graded expression (Fig. 3A). Higher magnification view shows that Wnt6 is enriched in barbule plate cells. This graded Wnt expression is similar to *Keratin-A*, which indicates terminal differentiation of the feather epithelium (Fig. 3A). Within each barb, the anterior barbule plate cells differentiate earlier than the posterior cells, as indicated by *Keratin-A* expression (Fig. S5).

The expression patterns of Wnt ligands and the receptor Fzd10 were examined by specific antibodies (Fig. 3B). Wnt6 was diffusive in early barbs, but was later enriched in barbule plate cells facing the axial plate (Fig. 3B). Similar expression pattern was found for Wnt5a (Fig. S6) and Fzd10 (Fig. 3B; quantified in Fig. 3D). The polarized distribution of Wnt ligands and the receptor suggests that they are upstream to control Pk1 localization and function. Indeed, when we perturbed the Wnt gradient by local injection of Wnt6 protein, barbule plate cells failed to change their shape and Pk1 asymmetric distribution was lost (Fig. 3C; quantified in Fig. 3D). Consistent with previous work (Yue et al., 2006), Wnt6 overexpression led to reduced barb growth, whereas a constitutively active β-catenin promoted barb growth (Fig. 3E). Thus it is crucial to coordinate the canonical and non-canonical pathways downstream of Wnt signaling. As expected, perturbation of the Wnt6 gradient leads to re-orientation of the feather branch (Fig. 3F). Similar results were also obtained for Wnt5a (Fig. S6; and the specificity of the antibodies were verified in Fig. S7). Thus the barb tilting is controlled by an anterior-posterior gradient of Wnt signaling as reported previously (Yue et al., 2006), and this regulation is via the function of Pk1 to coordinate cell shape change.

The apical-basal polarity of barbule plate cells controls the asymmetric localization of Wnt/Fzd and Pk1

We asked how the polarized distribution of Wnt6 and Fzd10 is achieved. Morphologically, it appears that the nuclei of barbule plate cells were localized at one side of the cells (Fig. S8), similar to the situation in polarized simple epithelium. We therefore examined the apical-basal polarity of these cells. It turns out that the molecular determinants of the apical compartment, Par3 and aPKC, are all localized facing the axial plate, suggesting that the barbule plate cells show apical-basal polarity in this tangential axis (Fig. 4A; quantified in Fig. 4C). To examine the functional significance of this polarity, we designed RNAi that effectively knockdown the expression of *Par3* and *aPKC*. This was confirmed both *in vitro* in DF-1 cells and *in vivo* in the developing feather follicle (Fig. S4). Knockdown of either *Par3* or *aPKC* led to failed cell shape change (Fig. 4B; quantified in Fig. 4C), dis-oriented barbs, and perturbed feather formation (Fig. S9). Furthermore, the polarized distributions of Fzd10 and Pk1 were also disrupted (Fig. 4D), and cell proliferation was inhibited (Fig. 4E). Finally, in radially symmetric feathers, the polarized localization of Par3/aPKC is readily established, whereas Fzd10 (Fig. 4F) and Pk1 (not shown) do not show polarization. These results suggest that the apical-basal polarity in barbule plate cells is upstream and controls the subsequent polarization of PCP pathway components.

DISCUSSION

The complex feather structure exemplifies how spatial forms are constructed via coordinated cell shape change. In feather development, there is a programmed change of cell shape: in early feather branches, the cells are almost round (length/width ration about 1), then gradually the barbule plate cells become elongated, and tilted in bilateral feathers. Our work illustrates how the Wnt signaling gradient is interpreted to coordinate this cell shape change and orient the feather branch. The PCP pathway is involved, which in turn is controlled by the Wnt/Fzd signaling. However, the polarized distribution of these core members is not according to the global Wnt gradient. Rather, their localization is determined locally within each barb, which is under the control of apical-basal polarity, namely the Par3/aPKC machinery (summarized in a hypothetical model Fig. 4G). In

radially symmetric feathers, the apical-basal polarity is readily established, however, there is no Wnt signaling gradient and thus no PCP activity to polarize the barbule plate cells. This is apparently due to the low levels of Wnt6/Wnt5a and Pk1, which showed graded expression in bilateral feathers and are only weakly expressed in radial feathers (Fig. S5).

The division of a continuous Wnt gradient into discrete signaling centers is due to the process of feather branching, which is mainly related to Notch and FGF signaling (Cheng et al., 2018). After branching, the marginal plate cells now directly face the pulp mesenchyme and become the basal epithelial cells. Thus the two columns of barbule plate cells acquire distinct apical-basal polarity, in opposite directions. The shape change of barbule plate cells is subsequent to this branching process. The fact that in radially symmetric feathers, the barbule plate cells do not tilt yet have an elongated shape suggests additional mechanisms independent of PCP to modulate the process. The PCP pathway kicks in relatively late to tilt the barbule cells and orient the feather branch. Nonetheless, the PCP pathway and Pk1 in particular can also modulate the shape of barbule plate cells, possibly because they can regulate the shared key cytoskeleton molecules. Indeed, *Pk1* knockout has been shown to disrupt the apical-basal polarity of mouse epiblast cells (Tao et al., 2009). To dissect the molecular mechanism of cell shape change in feather development, which is specifically in barbule plate cells but not marginal plate nor axial plate cells, precise gene manipulation in these different cell populations is required. Future work to characterize specific promoters for these different cell populations will be essential to design such experiments.

There are subtle differences among manipulating the different aspects of Wnt signaling in feather development, such as *Pk1* knockdown/Wnt6 overexpression/β-*catenin* overexpression. It appears β-catenin promotes barbule cell growth (Fig. 3E). On the other hand, Wnt6 overexpression inhibited barb growth, which is consistent with our previous work that Wnt3a overexpression does not elongate the barbule but disrupts barb patterning (Yue et al. 2006). The downstream events of Wnt signaling are complex and multi-faced. It is possible that Wnt overexpression triggers cell differentiation through the

Wnt/Calcium pathway. The details will need further investigation. On the other hand, the patterning of barb ridges was disrupted in all samples (*Par3*-RNAi, *PRKCI*-RNAi, *Wnt6*-OE, and *Pk1*-RNAi; Fig. S10). One reason could be that cell shape change requires the function of these molecules (thus no distinct after their perturbation). The reduced cell number (as is the case of *Par3*-RNAi, *PRKCI*-RNAi, *Wnt6*-OE, and to a less extent, *Pk1*-RNAi) may inhibit the branching process as well, in addition to patterning the barb ridge. However, it remains unknown how the barb ridge is patterned: that is, specification of the marginal plate cells, barbule plate cells and axial plate cells. This question also requires further investigation.

It is likely that the preferential localization of Wnt/Fzd proteins in the apical side of the barbule plate cells is controlled by the directional transportation/retention mechanisms associated with the apical-basal machinery (Roman-Fernandez and Bryant, 2016; Galic and Matis, 2015; Lee and Streuli, 2014). Although the details remain unclear at this moment, our preliminary results showed that by destabilizing the microtubule network via colchicine treatment, the polarized distribution of Par3/Wnt6/Fzd10 were all disrupted (data not shown). In summary, our results reveal a new strategy through which the global morphogen gradient is interpreted locally, thus coordinate the construction of complex spatial structures.

MATERIALS AND METHODS

Experimental animals

Adult male chicken (*Gallus gallus domesticus*) aged 3-6 months were purchased from local farms and housed in the animal facility of Fuzhou University with free access to food and water. All experimental protocols were approved by Fuzhou University Experimental Animal Ethics Board. For feather plucking and virus injection into the follicle cavity, anesthesia was not necessary; for virus injection into the growing follicle and collection of regenerating follicles, chickens were anesthetized by intraperitoneal injection of pentobarbital at 50mg/kg body weight.

Immunohistochemistry, immunofluorescence, and in situ hybridization

Feather samples were fixed in PBS solution containing 4% parafomaldehyde. Samples were then processed for paraffin embedding and sectioned at 6μm. Standard protocol for hematoxylin-eosin staining was used. For imunofluorescence staining, antigen retrieval was performed using 10mM citrate buffer pH6.0. After staining, the slides were counterstained with 1μg/ml DAPI, mounted and photographed using a Leica fluorescence microscope. Antibodies used: chicken Prickle1 (home made; see Supplemental Methods and Fig. S2; 1:100 dilution), β-Catenin (Sigma, Shanghai, China; C2206, 1:200 dilution), PCNA (Santa Cruz, Dallas, USA; sc-7907, 1:200 dilution); Wnt6 (Protentech, Wuhan, China; 24201-1-AP; 1:200 dilution), Wnt5a (Protentech, Wuhan, China; 55184-1-AP; 1:200 dilution), Fzd10 (Protentech, Wuhan, China; 18175-1-AP; 1:200 dilution), Par3 (Protentech, Wuhan, China; 11085-1-AP; 1:200 dilution), aPKC (Protentech, Wuhan, China; 13883-1-AP; 1:200 dilution). Method for in situ hybridization has been described previously (Chu et al., 2014). Probes used: *Prickle1* (nt1532-2187; XM_416036.5), *Wnt5a* (nt 382-1208; NM_204887.1), *Wnt6* (nt 191-507; NM_001007594.2), *Keratin-A* (nt 158-708; NM_001101732.2).

Lentiviral production and RNAi knockdown

Standard protocol for lentiviral production using 293T cells were followed and has been described previously (Chu et al., 2014). We used the pLL3.7 vector to construct shRNA for gene knockdown. Target sequences for chicken *Prickle1*: 5'-ATCCAAGAGCTGGACATG-3', *Par3*: 5'- ACAGGAGACGTACTTACA-3'; *aPKC*: 5'- AAGTGTCACAAACTGGTC-3'. A scramble control was constructed with the target sequence 5'-AGATACGACAGAGGACACT-3'. To monitor the RNAi knockdown efficiency, constructs were transfected into the chicken fibroblast cell line DF-1 (Cell Library of the Chinese Academy of Sciences, Shanghai, China, #GNO30) using Lipofectamine 2000, and cells were harvested 48 hours post-transfection. Total RNAs were extracted and processed for RT-PCR and qPCR analysis (Roche LightCycler 480). To monitor the knockdown efficiency in vivo, the follicles were plucked, infected with the virus, and collected 4 days later. Total RNAs were extracted for gene expression analysis. In addition, the developing feather follicles were locally injected with the virus,

and samples were collected 2-days later and stained for protein expression. Virus infection was confirmed by the GFP expression carried on the viral vector. Primers used: β-*Actin* (forward 5'- CTGACGGACTACCTCATGAA-3', reverse 5'- CCTCTCATTGCCAATGGTGA-3'); *Prickle1* (forward 5'- AGAAGATCTAAATCCCAGTCT-3', reverse 5'- GTGATCCTGAGGTGAGTAAT-3'); *Par3* (forward 5'- CTCCTAACAATCATGACCGG-3', reverse 5'- CTTGTCGTTGCCGTTGCATT-3'); *aPKC* (forward 5'- ATCCAAAGGAGCGGTTAGGC-3', reverse 5'- GCTGCACAGGTTCATTGGTG-3').

***In vivo* gene transfer and protein injection in the feather follicle**

For virus infection of the regenerating feather follicle, feathers were plucked and 100~200μL virus solution was injected into the follicle cavity. Feathers were collected 1~2 months later to examine the morphological changes. For virus injection into the growing feather follicle, a small hole was punched in the follicle wall near the base of the follicle, and 2-3μL virus solution was injected using a fine glass needle. Samples were collected 48 hours post-injection to visualize the disrupted branches. Similar procedures were adopted for protein injection into the feather follicle. Plasmids containing Wnt5a or Wnt6 under the control of a CMP promoter in pEGFP vector were overexpressed in 293T cells. The cells were harvested by trypsin/EDTA digestion, and sonicated before injection. Non-transfected cells were used as control. For β-catenin overexpression, a constitutively active form of β-catenin was cloned into the RCAS vector and infected the feather follicle (Widelitz et al., 2000). Samples were collected two weeks later for histological analysis.

Documentation of the feather morphology

Feather morphology was photographed using a Leica stereo 3D microdissection microscope. To visualize the developing feather branches, feathers were plucked and cut open under a dissection microscope (Yue and Xu, 2017). After removing the pulp mesenchyme, the epithelium was fixed by 4% PFA at 4^0C overnight, counterstained by 1 ug/ml DAPI in PBS for 1 hour at room temperature, briefly washed in 3X PBS, and mounted for photograph under an inverted Nikon fluorescence microscope.

Quantification of feather morphological characteristics

Wing contour feathers and leg feathers in adult chicken were used as bilateral and (nearly) radial feathers. Feathers were plucked to induce regeneration for about 2 weeks and collected, which is in active growing phase. The early, middle and later stages of barb maturation were defined as following: starting from the initial branching, every 30 sections (6μm thick) were collected, which correspond to about 200μm in distance. The tilting angle of barbule plate cells were measured (using Adobe Illustrator CS6) for both the anterior (αA) and posterior (αP) column of cells, with reference to the horizontal line as the tangential line of the follicle circle. The length and width of barbule plate cells were also measured (in Adobe Illustrator CS6) from at least three barbs, and at least twenty cells. The asymmetry index (ASI) is defined as (A-P)/(A+P), where A, P define the anterior and posterior signal, respectively. The anterior and posterior signals are measured separately by using the ImageJ program after bi-sect the cells into the anterior and posterior halves (Rodriguez et al., 2017; Fig. S2).

Statistics

Each experiment was repeated at least three times. For gene transfer in the feather follicle, at least 15 follicles were each individually manipulated. Data shown were mean ± standard error (se). The statistical difference between two groups was determined by the two-tailed *t*-test, and the *p*-value was calculated.

Acknowledgements

We thank Drs Cheng-Ming Chuong and Randall Widelitz (University of Southern California, Los Angeles, USA) for the helpful input, and Zhang Juan for technical assistance.

Author contributions

ZY conceived the work. JL performed the experiments. ZY and JL wrote the paper.

Competing interests

The authors declare no competing or financial interests.

Funding

This work is supported by start-up funds from Fuzhou University, and NSFC 31071285, 81673094.

Supplementary information

Supplementary information is available online.

References

Akiyama, T. and Gibson, M.C. (2015). Morphogen transport: theoretical and experimental controversies. *Wiley Interdiscip. Rev. Dev. Biol*. **4**, 99-112.

Aw, W.Y. and Devenport, D. (2017). Planar cell polarity: global inputs establishing cellular asymmetry. *Curr. Opin. Cell Biol*. **44**, 110-116.

Boutros, M. and Niehrs, C. (2016). Sticking around: short-range activity of Wnt ligands. *Dev. Cell* **36**, 485-486.

Chen, C.F., Foley, J., Tang, P.C., Li, A., Jiang, T.X., Wu, P., Widelitz, R.B. and Chuong, C.M. (2015). Development, regeneration, and evolution of feathers. *Annu. Rev. Anim. Biosci.* **3**, 169-195.

Chen, X., Liao, C., Chu, Q., Zhou, G., Lin, X., Li, X., Lu, H., Xu, B. and Yue, Z. (2014). Dissecting the molecular mechanism of ionizing radiation-induced tissue damage in the feather follicle. *Plos One* **9**, e89234.

Cheng, D, Yan, X., Qiu, G., Zhang, J., Wang, H., Feng, T., Tian, Y., Xu, H., Wang, M., He, W. et al. (2018). Contraction of basal filopodia controls periodic feather branching via Notch and FGF signaling. *Nat. Commun*. **9**, 1345.

Chu, Q., Cai, L., Fu, Y., Chen, X., Yan, Z., Lin, X., Zhou, G., Han, H., Widelitz, R.B., Chuong, C.M. et al. (2014). Dkk2/Frzb in the dermal papilla regulates feather regeneration. *Dev. Biol*. **387**, 167-178.

Farin, H.F., Jordens, I., Mosa, M.H., Basak, O., Korving, J., Tauriello, D.V., de Punder, K., Angers, S., Peters, P.J., Maurice, M.M. and Clevers, H. (2016). Visualization of a short-range Wnt gradient in the intestinal stem-cell niche. *Nature* **530**, 340-343.

Feo, T.J., Simon, E. and Prum, R.O. (2016). Theory of the development of curved barbs and their effects on feather morphology. *J. Morphol*. **277**, 995-1013.

Galic, M. and Matis, M. (2015). Polarized trafficking provides spatial cues for planar cell polarization within a tissue. *Bioessays* **37**, 678-686.

Gao, B., Song, H., Bishop, K., Elliot, G., Garrett, L., English, M.A., Andre, P., Robinson, J., Sood, R., Minami, Y., et al. (2011). Wnt signaling gradients establish planar cell polarity by inducing Vangl2 phosphorylation through Ror2. *Dev. Cell* **20**, 163-176.

Gao, B. and Yang, Y. (2013). Planar cell polarity in vertebrate limb morphogenesis. *Curr. Opin. Genet. Dev.* **23**, 438-44.

Hamada, H., Watanabe, M., Lau, H.E., Nishida, T., Hasegawa, T., Parichy, D.M. and Kondo, S. (2014). Involvement of Delta/Notch signaling in zebrafish adult pigment stripe patterning. *Development* **141**, 318-324.

Kornberg, T.B. and Roy, S. (2014). Cytonemes as specialized signaling filopodia. *Development* **141**, 729-736.

Lander, A.D. (2007). Morpheus unbound: reimagining the morphogen gradient. *Cell* **128**, 245-256.

Lee, J.L. and Streuli, C.H. (2014). Integrins and epithelial cell polarity. *J. Cell Science* **127**, 3217-3225.

Li, A., Figueroa, S., Jiang, T.X., Wu, P., Widelitz, R., Nie, Q. and Chuong, C.M. (2017). Diverse feather shape evolution enabled by coupling anisotropic signalling modules with self-organizing branching programme. *Nat. Commun*. **8**, 14139.

Lin, S.J., Wideliz, R.B., Yue, Z., Li, A., Wu, X., Jiang, T.X., Wu, P. and Chuong, C.M. (2013). Feather regeneration as a model for organogenesis. *Dev. Growth Differ*. **55**, 139-148.

Lucas, A.M. and Stettenheim, P.R. (eds). (1972). Avian anatomy-integument. Agriculture Handbook. U.S. Department of Agriculture, Washington DC, USA.

Nahmad, M. and Lander, A.D. (2011). Spatiotemporal mechanisms of morphogen gradient interpretation. *Curr. Opion Genet. Dev*. **21**, 726-731.

Rodriguez, J., Peglion, F., Martin, J., Hubatsch, L., Rech, J., Hirani, N., Gubieda, A.G., Rofffey, J., Fernandes, A.R., St Johnston, D., et al. (2017). aPKC cycles between functionally distinct PAR protein assemblies to drive cell polarity. *Dev. Cell* **42**, 400-415.

Roman-Fernandez, A. and Bryant, D.M. (2016). Complex polarity: building multicellular tissues through apical membrane traffic. *Traffic* **17**, 1244-1261.

Prum, R.O. (2005). Evolution of the morphological innovations of feathers. *J. Exp. Zool. B Mol. Dev. Evol*. **304**, 570-579.

Prum, R.O. and Williamson, S. (2001). Theory of the growth and evolution of feather shape.*J. Exp. Zool*. **291**, 30-57.

Sagner, A. and Briscoe, J. (2017). Morphogen interpretation: concentration, time, competence, and signaling dynamics. *Wiley Interdiscip. Rev. Dev. Biol*. **6**, e271.

Sanders, T.A., Llagostera, E. and Barna, M. (2013). Specialized filopodia direct long-range transport of SHH during vertebrate tissue patterning. *Nature* **497**, 628-632.

Widelitz, R.B., Jiang, T.X., Lu, J., and Chuong, C.M. (2000). beta-catenin in epithelial morphogenesis: conversion of part of avian foot scales into feather buds with a mutated beta-catenin. *Dev. Biol*. **219**, 98-114.

Xie, G., Wang, H., Yan, Z., Cai, L., Zhou, G., He, W., Paus, R. and Yue, Z. (2015). Testing chemotherapeutic agents in the feather follicle identifies a selective blockade of cell proliferation and a key role for sonic hedgehog signaling in chemotherapy-induced tissue damage. *J. Invest. Dermatol*. **135**, 690-700.

Yang, Y. and Mlodzik, M. (2015). Wnt-Frizzled/planar cell polarity signaling: cellular orientation by facing the wind (Wnt). *Annu. Rev. Cell Dev. Biol*. **31**, 623-646.

Yu, M., Yue, Z., Wu, P., Wu, D.Y., Mayer, J.A., Medina, M., Widelitz, R.B., Jiang, T.X. and Chuong, C.M. (2004). The biology of feather follicles. *Int. J. Dev. Biol*. **48**, 181-191.

Yue, Z., Jiang, T.X., Widelitz, R.B. and Chuong, C.M. (2006). Wnt3a gradient converts radial to bilateral feather symmetry via topological arrangement of epithelia. *Proc. Natl. Acad. Sci. USA* **103**, 951-955.

Yue, Z. and Xu, B. (2017). The feather model for chemo- and radiation therapy-induced tissue damage. In: Sheng G. (eds) Avian and reptilian developmental biology. *Methods Mol. Biol*. **1650**, 299-307 (Humana Press, New York, NY).

Zallen, J.A. (2007). Planar polarity and tissue morphogenesis. *Cell* **129**, 1051-1063.

Figures

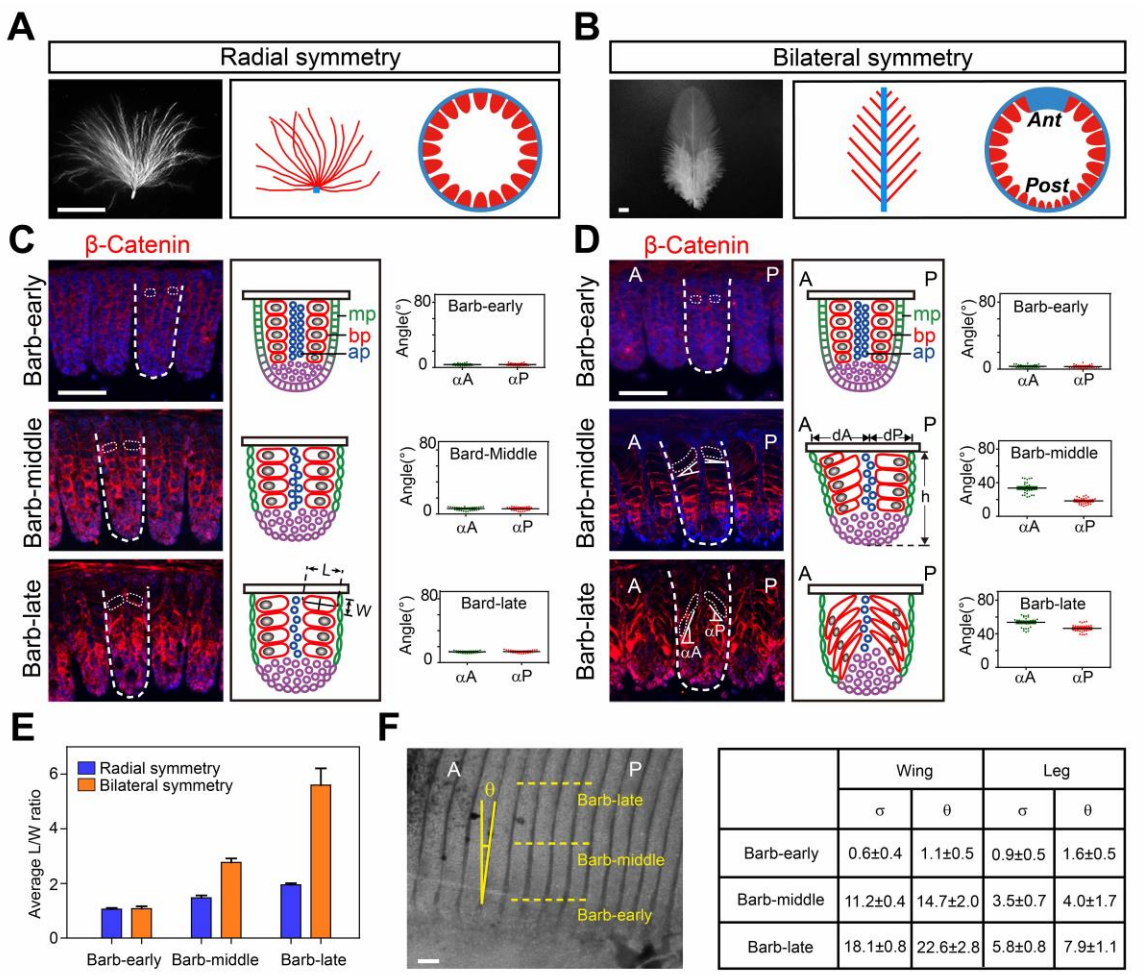

	Wing		Leg	
	σ	θ	σ	θ
Barb-early	0.6±0.4	1.1±0.5	0.9±0.5	1.6±0.5
Barb-middle	11.2±0.4	14.7±2.0	3.5±0.7	4.0±1.7
Barb-late	18.1±0.8	22.6±2.8	5.8±0.8	7.9±1.1

Fig. 1. Coordinated cell shape change in feather development. (A-B) Morphology of radial (A) and bilateral (B) feathers. In radial feathers, the barbs attach to the calamus parallelly. In bilateral feathers, there is a central rachis which is the anterior of the follicle. The barbs attach to the rachis helically. (C-D) β-Catenin/DAPI staining showing the cell shape change in radial (C) and bilateral (D) feathers. Continuous sections were collected to show the early, middle and late stage of barb maturation along the proximal-distal axis of the follicle (illustrated in panel F). The marginal plate (mp, green), barbule plate (bp, red) and axial plate (ap, blue) cells in each barb ridge were shown in diagrams. The coordinated cell shape change creates a disparity in the width of the two columns of barbules, dA/dP. The height (h) of the barb is also depicted. The length-width (L-W) of

barbule plate cells and their tilting angles (αA and αP) are quantified. (E) Quantification of barbule plate cell shape change by their length and width (L/W) ratio. (F) Comparison of the actual barb tilting angle θ and the calculated tilting angle σ = arctg[(dA-dB)/h]. Wing contour feathers and leg feathers in adult chicken were used for bilateral and (nearly) radial feathers. Scale bars: 5mm in A, B; 50μm in C, D, F.

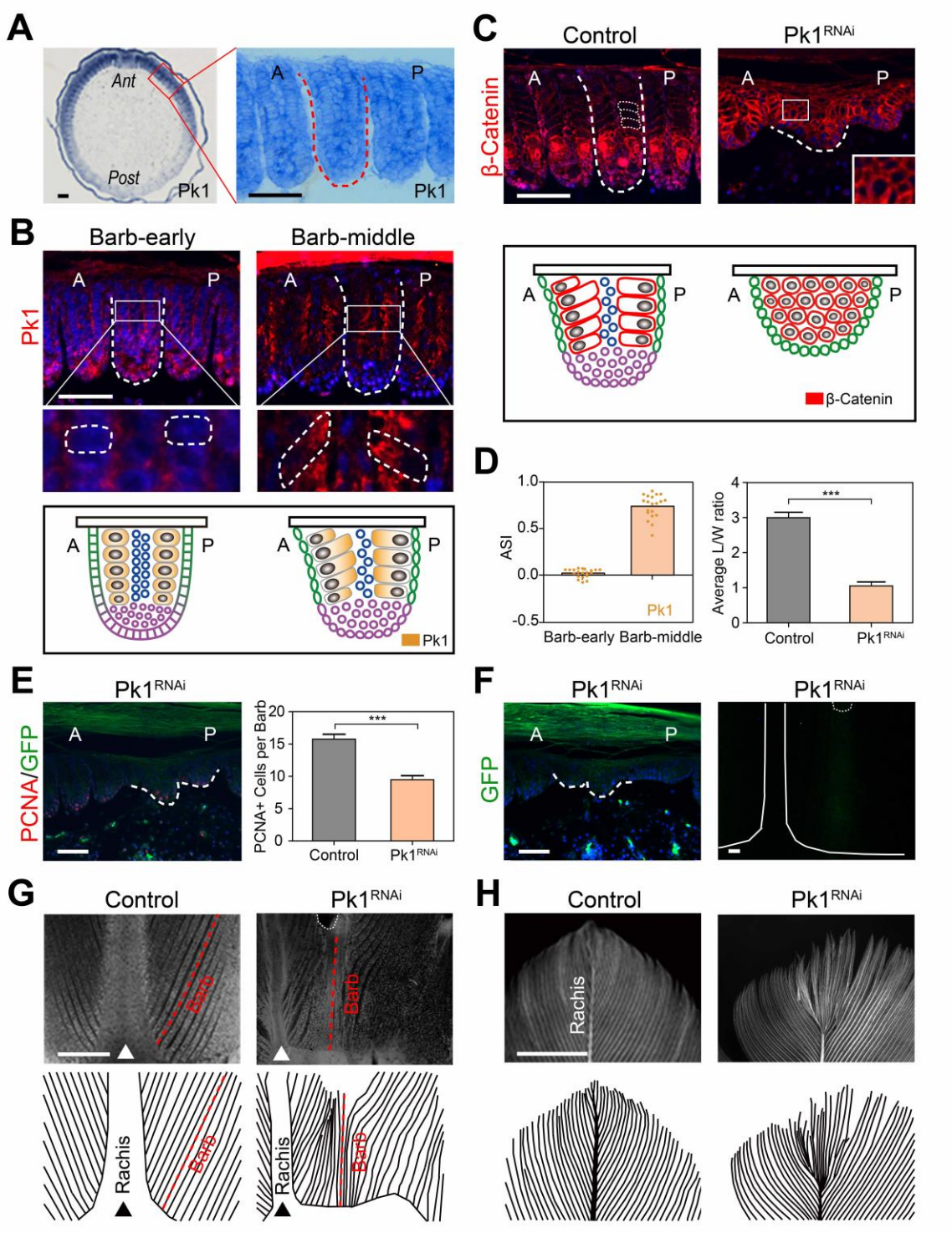

Fig. 2. Pk1 regulates cell shape change and barb tilting. (A) In situ hybridization showing the anterior-posterior gradient of *Pk1* expression. (B) Immunostaining showing the initial homogenous distribution of Pk1, which gradually enriched toward the axial plate. (C) RNAi knockdown of *Pk1* resulted in failed cell shape change in the barb ridge. (D) Quantification of Pk1 asymmetric distribution and cell shape change. (E) *Pk1* knockdown reduced barb cell proliferation as quantified by PCNA staining. GFP expression indicated virus expression. (F) Virus expression after local injection as monitored by GFP levels. (G) Failed barb tilting after *Pk1* knockdown. (H) *Pk1* knockdown promoted transition toward radial symmetry in the feather morphology. ***, $p < 0.001$. Scale bars: 50μm in A-C, E, F; 200μm in G, 1cm in H.

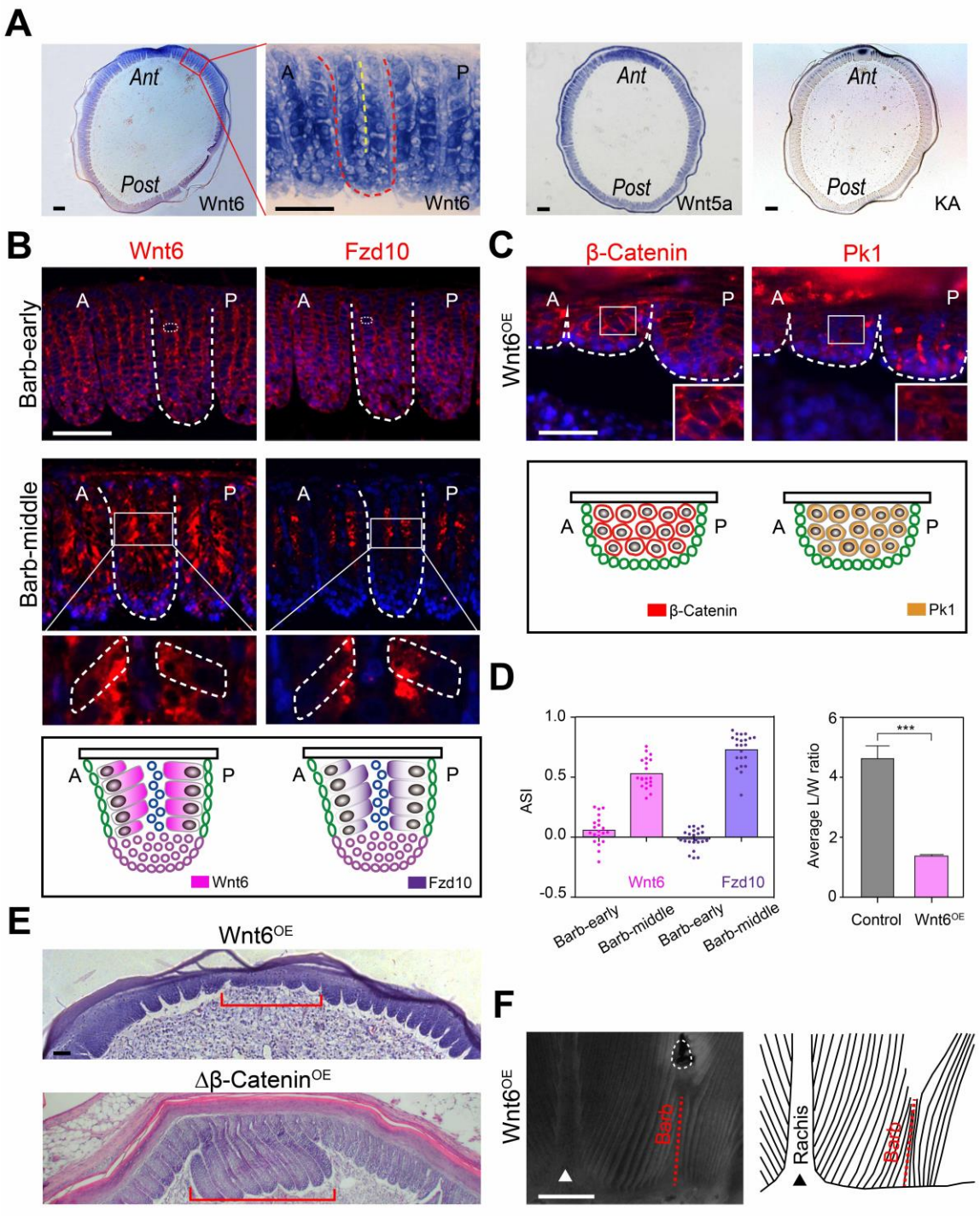

Fig. 3. The Wnt6/Fzd10 signaling regulates Pk1 asymmetric distribution and cell shape change. (A) In situ hybridization showing the graded expression of *Wnt6*, *Wnt5a* and the differentiation marker *Keratin-A* (*KA*). (B) Immunostaining of Wnt6 and Fzd10. Both showed polarized expression in the barbule plate cells, with the highest expression facing the axial plate. (C) Disruption of the Wnt gradient by local injection of Wnt6 led to diffusive Pk1 expression and failed cell shape change. (D) Quantification of Wnt6 and Fzd10 asymmetry and barbule cell shape change. (E) Wnt6 overexpression reduced barb growth, whereas overexpression of a constitutively active β-catenin promoted barb growth. (F) Failed barb tilting after locally overexpress Wnt6. ***, $p < 0.001$. Scale bars: 50μm in A-C and E, 200μm in F.

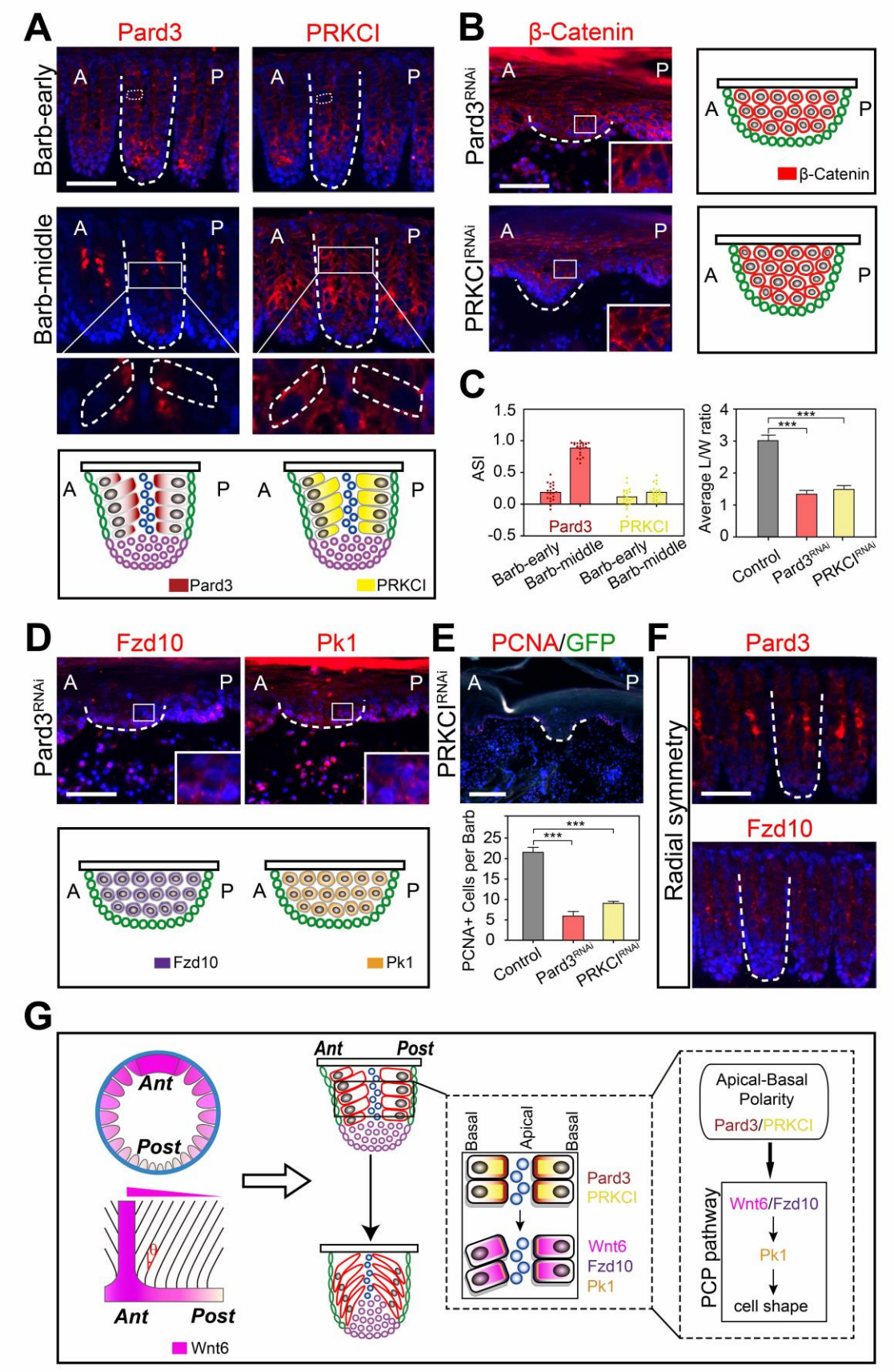

Fig. 4. The apical-basal polarity of barbule plate cells controls polarized distribution of Wnt/Fzd and Pk1. (A) Par3 and aPKC were polarized in the barbule plate cells. (B) Knockdown of *Par3* or *aPKC* resulted in irregular feather branching and failed cell shape change. (C) Quantification of Par3 and aPKC asymmetric distribution, and cell shape change. (D-E) Knockdown of *Par3* or *aPKC* disrupted Fzd10 and Pk1 localization (D), and reduced cell proliferation (E). (F) In radial feathers, Par3 is polarized but Fzd10 failed to polarize in barbule plate cells. (G) A hypothetical diagram showing the apical-basal polarity machinery Par3/aPKC controls the localization of Wnt6/Fzd10, which then regulates Pk1 polarization and function. These events are independently regulated locally within each barb and are not according to the global Wnt gradient. ***, $p < 0.001$. Scale bars: 50μm.

Supplementary Information

Supplementary methods

Production and affinity-purification of the chicken Prickle1 antibody.

A segment at the C-terminus (amino acid 512-801; protein ID: XP_416036.2) of the chicken *Prickle1* gene was PCR cloned into the expression vector pET-32a, using the following primer pair: sense 5'-GGTACGGAGGTTCACTTGAA-3', antisense 5'-GATAACGCAGTAGTTGGACC-3'. Protein expression was induced by 1mM IPTG in BL21 bacteria. The Hig-tag fusion protein was affinity purified by a Nickel resin column (GeneScript). The purified lysate was further concentrated by running a SDS-PAGE gel and cut off the band at the correct size. The gel band was then used to immunize the mice with Freud's adjuvant (Sigma). The antiserum was collected and affinity purified by using the Prickle1-conjugated Nickel resin column.

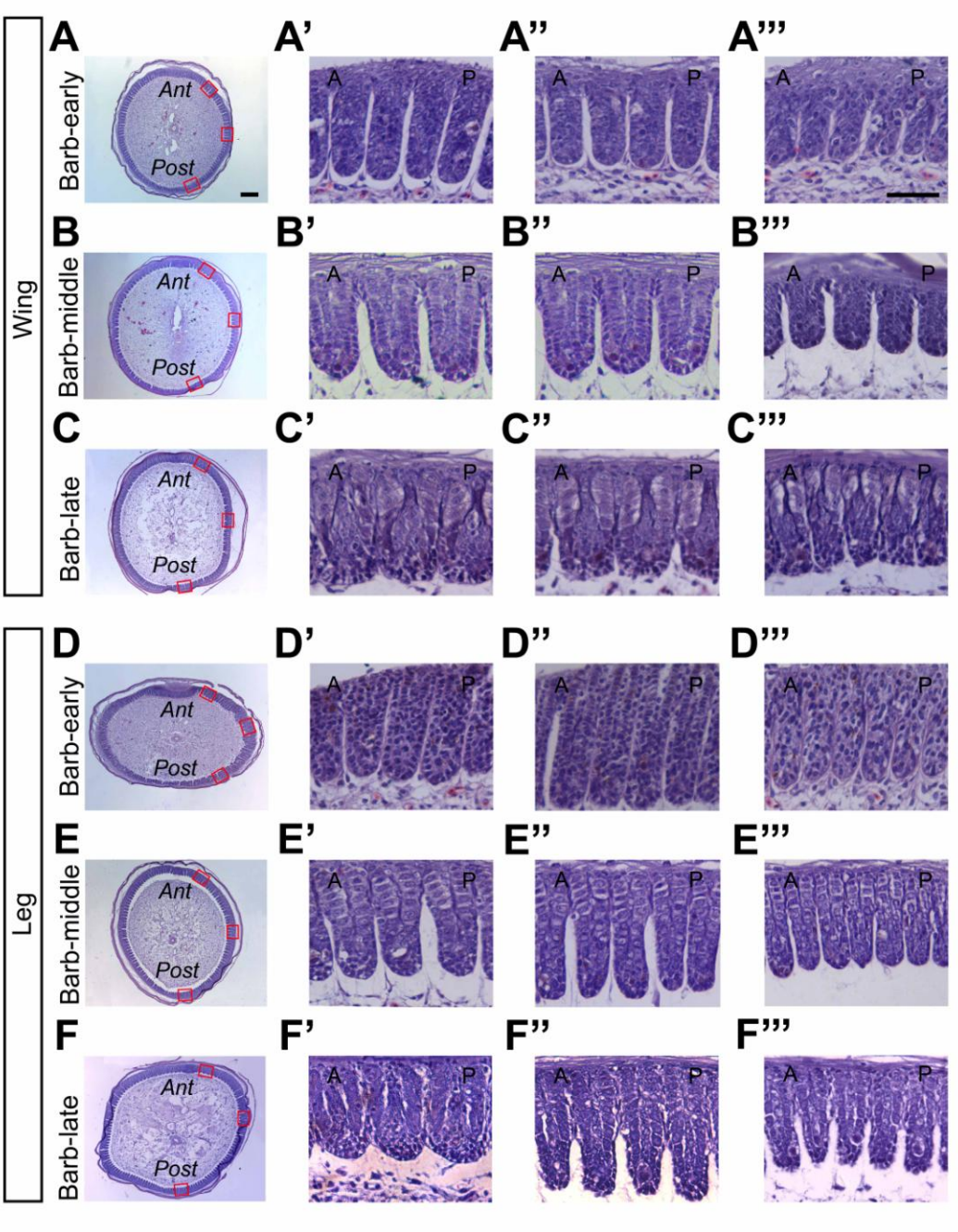

Fig. S1. Additional analysis of cell shape change in feather development. (A-C) Wing contour feathers as bilateral feathers. (D-F) Leg feathers as an approximation of radial feathers. The anterior, middle and posterior regions (red boxes) are shown as enlarged images. In bilateral feathers, the anterior barbule cells are elongated earlier, but eventually the posterior barbule cells are also elongated. This is in contrast to the radial feathers where the posterior barbule cells do not elongate. Scale bar: 50μm.

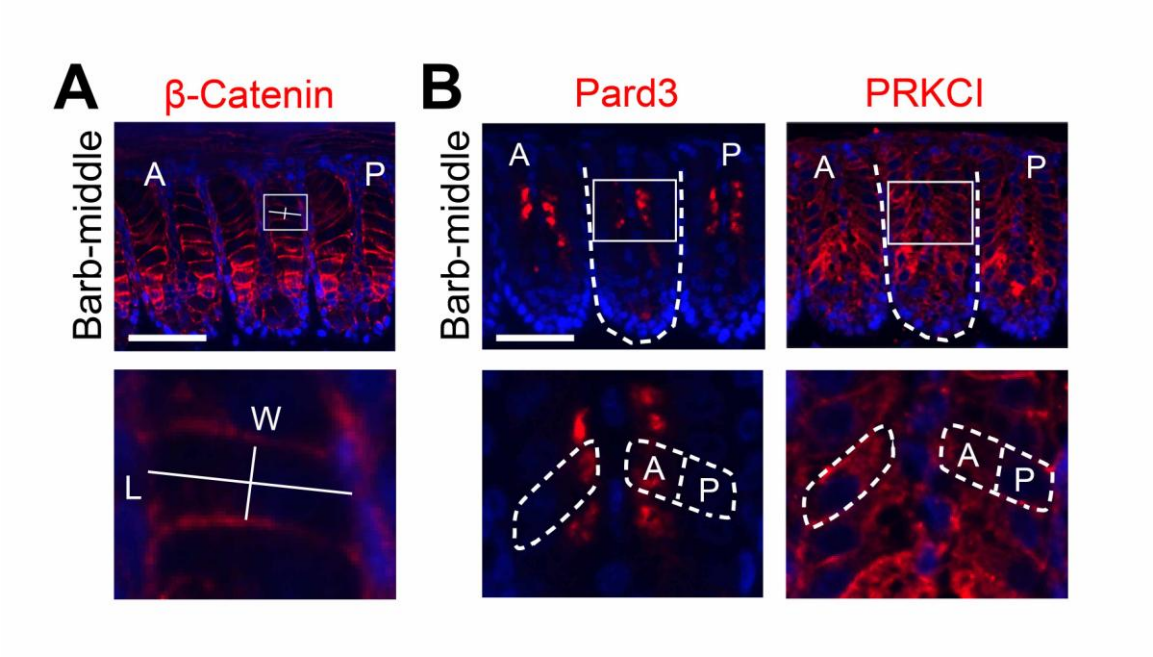

Fig. S2. Diagrams showing the measurement of barbule cell parameters. (A) The length (L) and width (W) of barbule plate cells. (B) The barbule cells were bisected into the anterior and posterior halves, and signal strengths were measured in each half using the ImageJ program. Scale bars: 50μm.

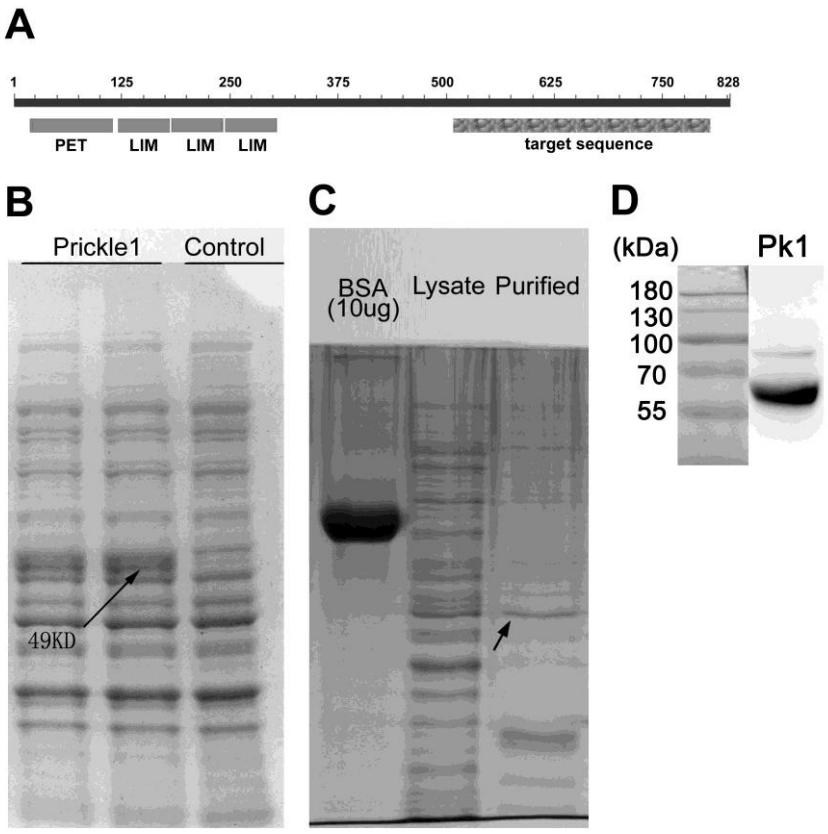

Fig. S3. Production and characterization of the chicken Pk1 antibody. (A) A segment near the C-terminus (amino acid 512-801) of chicken *Prickle1* gene was cloned into the pET-32a vector and expressed in BL-2 bacteria. (B) SDS-PAGE gel showing the induced expression of fusion protein by 1mM IPTG, which has the predicted size. (C) The fusion protein was purified using a Ni column. This protein was further concentrated by SDS-PAGE gel and the band was cut off at the predicted size to immunize the mice. (D) After purification, the antibody was verified in whole-feather lysate by Western blot analysis. A strong band at about 60kd was detected, as well as a weaker band at about 90kd, possibly corresponding to the different isoforms of this protein (similar to the Proteintech antibody 22589-1-AP and Abcam antibody #139077).

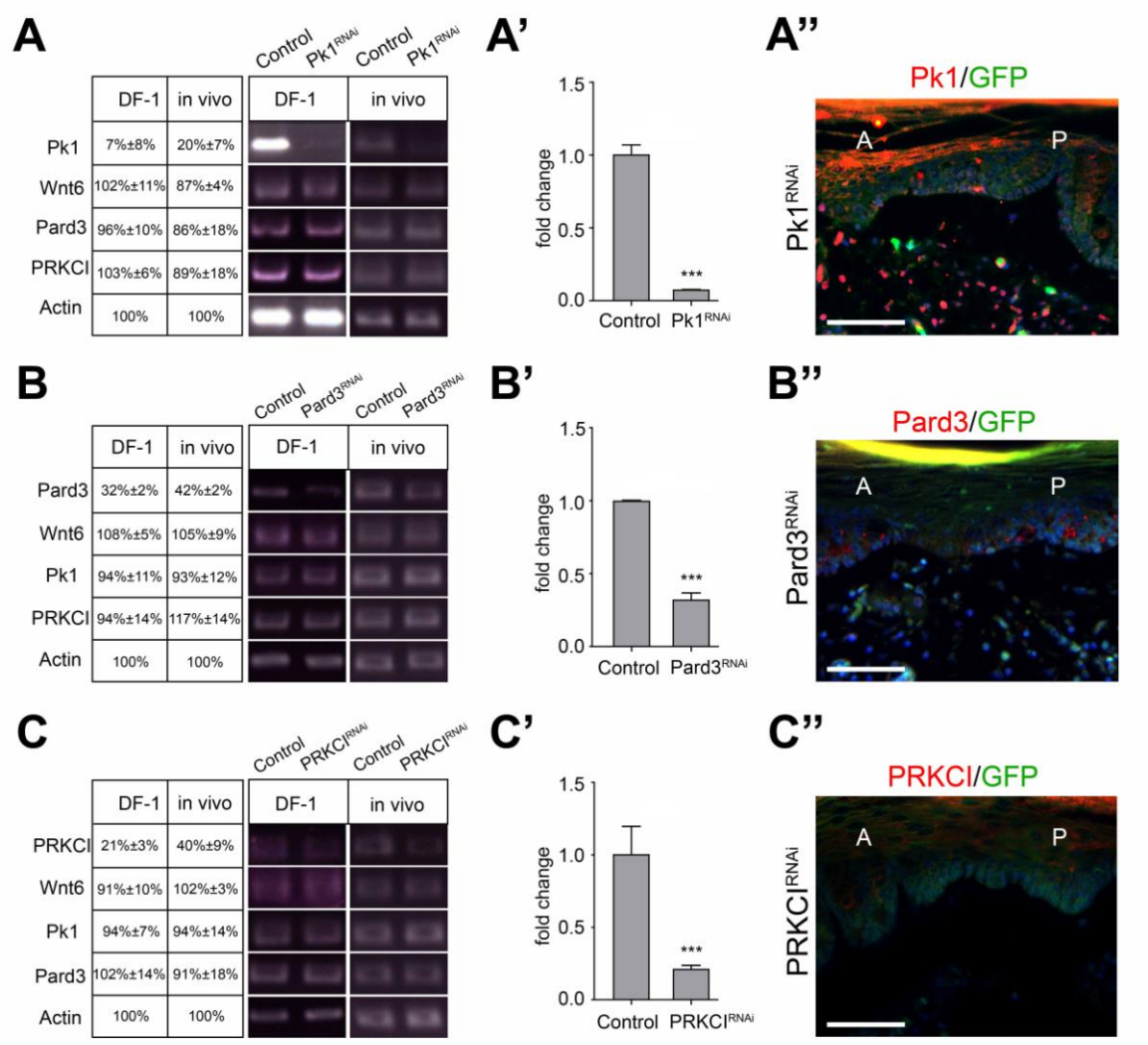

Fig. S4. The RNAi knockdown efficiency as examined both in vitro and in vivo. (A) Pk1, (B) Par3, and (C) aPKC. The constructs were transfected into DF-1 cells for 48 hours, or infect the feather follicle for 4 days before sample collection. A scramble viral vector was used as control. Gene expression levels were monitored by semi-quantitative RT-PCR and further quantified by qRT-PCR (A', B', C'; results are from DF-1 cells). In addition, local injection of the virus into the developing follicles were performed, and samples were collected 2 days later to examine the protein expression (red) and virus expression (GFP; A'', B'', C''). ***, $p < 0.001$. Scale bars: 50μm.

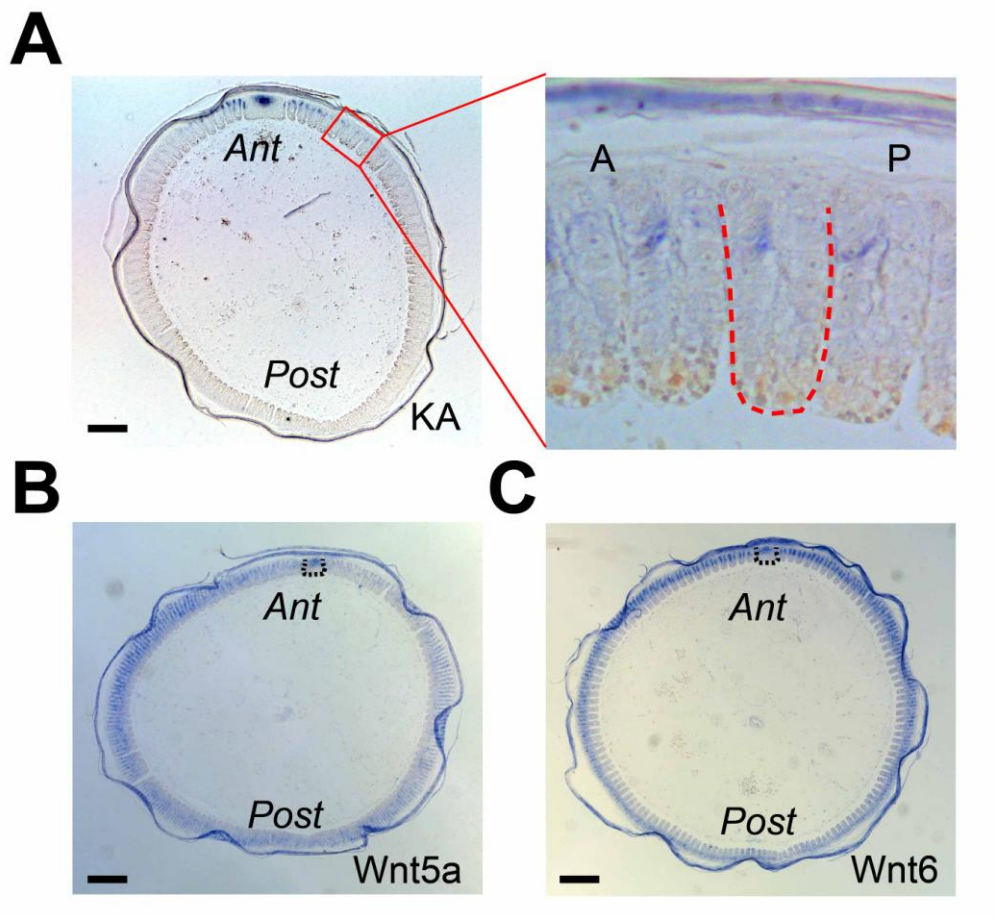

Fig. S5. Characterization of molecular expression in the feather follicle. (A) *Keratin-A* (*KA*) expression in bilaterally symmetric feathers. *KA* is expressed in the anterior barbule plate cells earlier than in the posterior barbule plate cells. (B-C) *Wnt5a* and *Wnt6* are weakly expressed in radially symmetric feathers. Scale bars: 100μm.

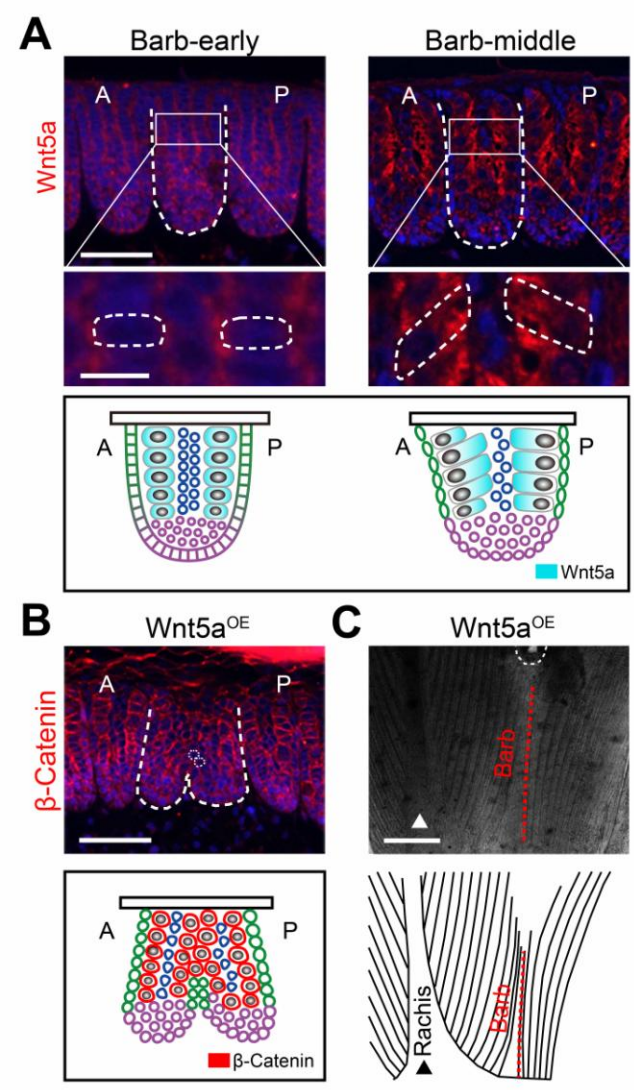

Fig. S6. Wnt5a expression and function in feather development. (A) Wnt5a was initially homogenously expressed, which then enriched toward the axial plate. (B) Overexpression of Wnt5a disrupted the programmed feather cell shape change. (C) Overexpression of Wnt5a disrupted directional tilting of barbs. Scale bars: 50μm in A, B; 200μm in C.

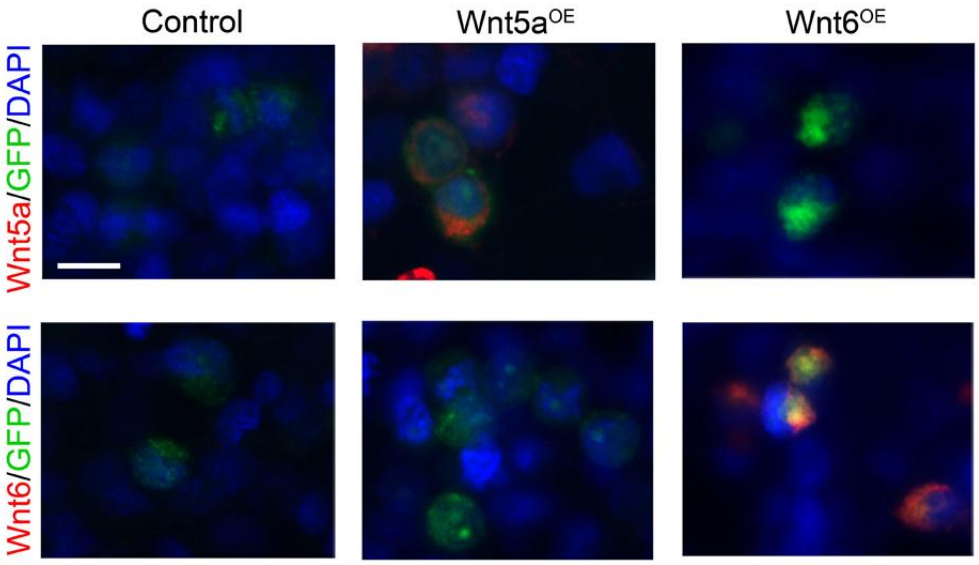

Fig. S7. Specificity of the antibodies for Wnt5a and Wnt6. The antibodies for Wnt5a and Wnt6 do not cross-react with each other. A control vector contains GFP is co-transfected into 293T cells, together with the plasmids containing the Wnt ligand Wnt5a or Wnt6, respectively. Scale bar: 20μm.

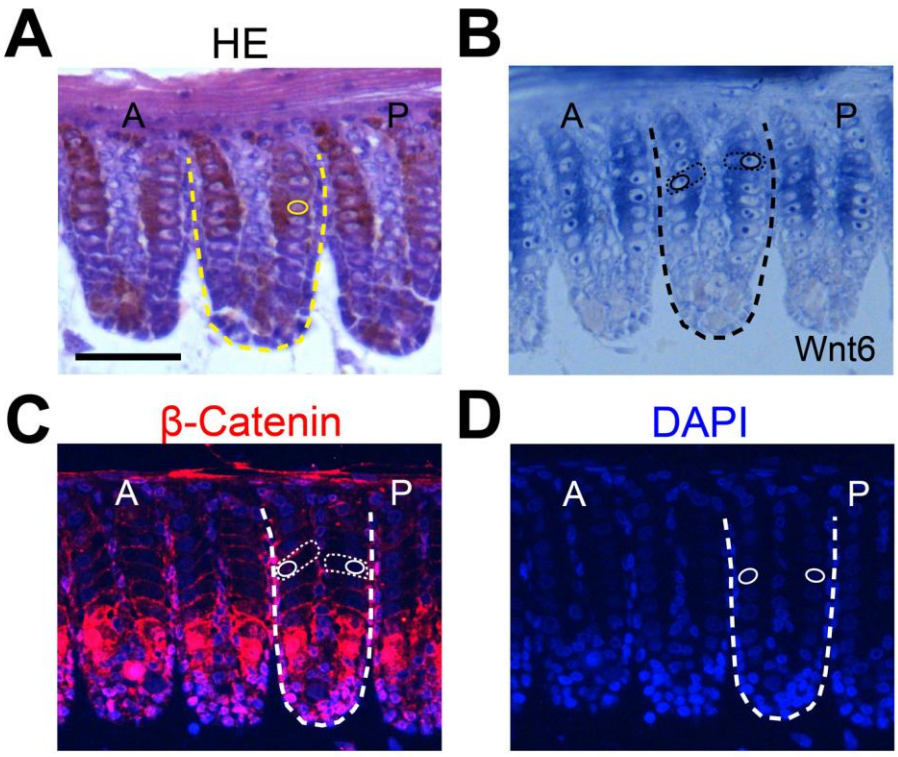

Fig. S8. Morphological features of apical-basal polarity in barbule plate cells. (A) HE staining of a pigmented feather (brown) showing the enrichment of cytoplasmic melanin content facing the axial plate, with the cell nucleus localized to the opposite side. (B) In situ hybridization of *Wnt6* showing the cytoplasmic mRNA in barbule plate cells were enriched facing the axial plate. (C-D) β-catenin and DAPI staining showing the relative localization of cell nuclei in barbule plate cells. Scale bar: 50μm.

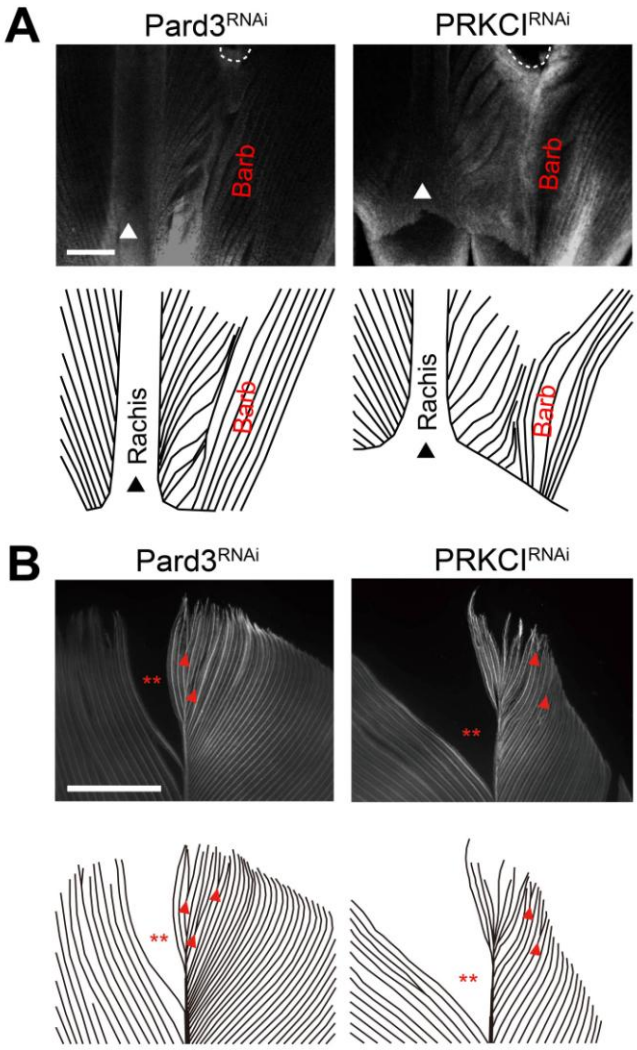

Fig. S9. Phenotypes of Par3 and aPKC perturbation. (A) Local perturbation of *Par3* or *aPKC* expression via injection of shRNA lentivirus disrupted barb tilting. (B) Gross morphology of feathers after knockdown of *Par3* or *aPKC* in vivo. Arrowheads, ectopic barb fusion; stars, regions showing lost of barbs. Scale bars: 200μm in A, 1cm in B.

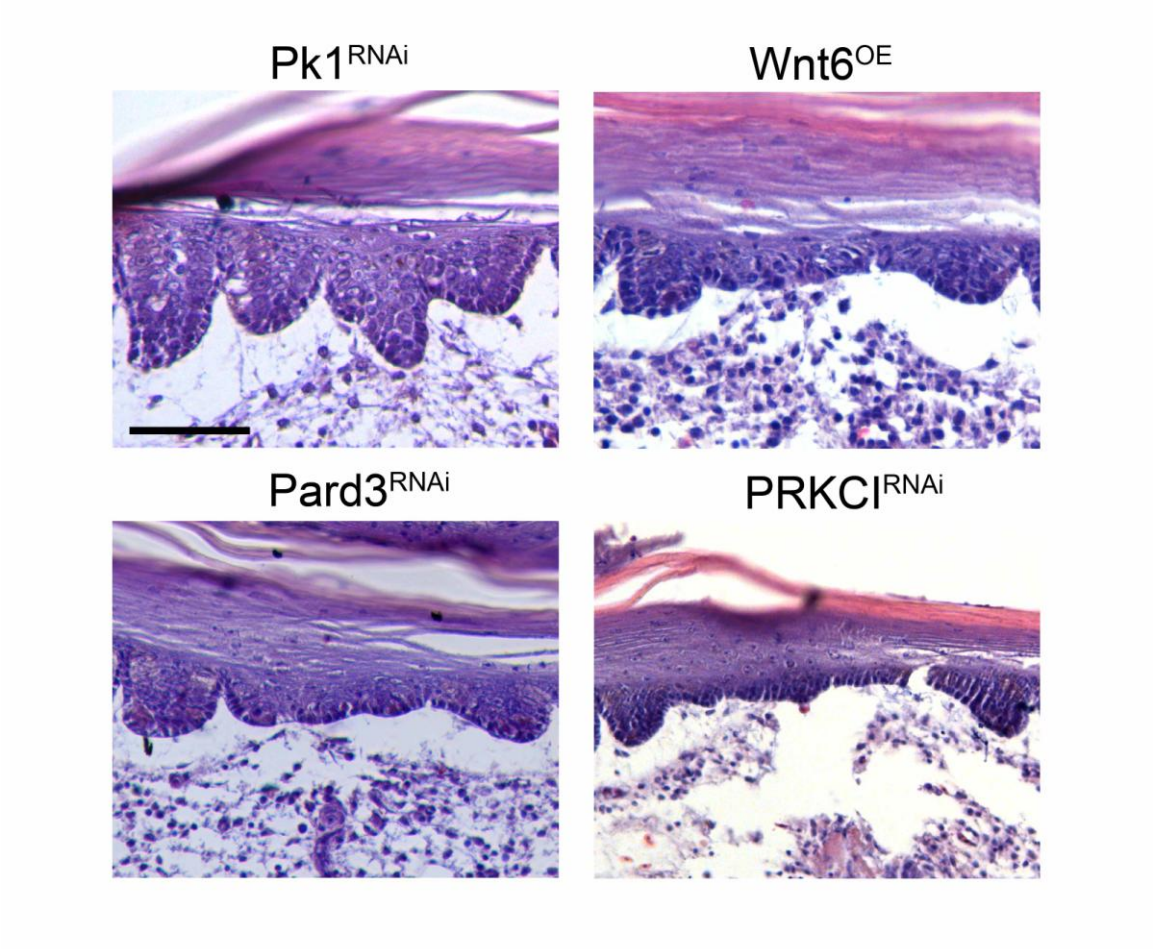

Fig. S10. Phenotypes of the feather barb after gene perturbation. Wnt6 overexpression (OE), Par3-RNAi or PRKCI-RNAi, and to a less extend Pk1-RNAi all reduced the cell number, and disrupted cell shape change within the barb. The branching of feather epithelium is also reduced/disrupted. Scale bar: 50μm.